

Paper:

Development of a Pneumatic Surgical Manipulator IBIS IV

Kotaro Tadano*, Kenji Kawashima*, Kazuyuki Kojima**, and Naofumi Tanaka**

*Precision and Intelligence Laboratory, Tokyo Institute of Technology
4259 Nagatsuta, Midori-ku, Yokohama-shi, 226-8503, Japan
E-mail: tadano@pi.titech.ac.jp

**Tokyo Medical and Dental University
1-5-45 Yushima, Bunkyo-ku, Tokyo 113-8519, Japan
[Received September 30, 2009; accepted January 25, 2010]

In teleoperated, minimally invasive surgery systems, the measurement and conveyance of a sense of force to the operator is problematic. In order to carry out safer and more precise operations using robotic manipulators, force measurement and operator feedback are very important factors. We previously proposed a pneumatic surgical manipulator that is capable of estimating external force without the use of force sensors. However, the force estimation had a sensitivity of only 3 N because of inertia and friction effects. In this paper, we develop a new and improved model of the pneumatic surgical manipulator, IBIS IV. We evaluate its performance in terms of force estimation. The experimental results indicate that IBIS IV estimates external forces with a sensitivity of 1.0 N. We also conduct an in-vivo experiment and confirm the effectiveness and improvement of the manipulator.

Keywords: surgical robot, force feedback, bilateral control, pneumatic servo system

1. Preface

Recent active developments of manipulators to assist surgical operations [1] are focused, among other things, on the development of various forceps manipulators with bending DOFs at the tip. This is in order to solve the problem of insufficient freedom extant in conventional surgical tools. There are two types of forceps manipulators: hand-held ones that are highly compatible with conventional surgical tools [2, 3] and master-slave systems [4–8].

The master-slave system, though a complex system, allows intuitive manipulation of surgical tools. To ensure more intuitive and much safer manipulation, presentation of contact force to operators is an indispensable function of the system [9–13].

The master-slave system often uses an electric motor with a reduction gear having a high reduction ratio to realize precise positioning. Low back-drivability of the electric motor will require a force sensor at the tip of the forceps to detect minute forces. In practice, however, a force sensor at the tip of the forceps is not desirable in terms of

miniaturization, sterilization, calibration, and cost. On the other hand, the use of direct-driven motors or geared motors with low reduction ratios will allow the estimation of external forces and the control of forces without the use of a force sensor [14, 15]. Such a motor, however, needs to be large enough to develop adequate drive torque, which makes it difficult to lighten or miniaturize the manipulator.

In such a context, we have worked on the development of a robotic system for laparoscopic surgery with 7-DOFs. In this system, pneumatic actuators, instead of electric motors, are used to detect external forces based on pressure values without a force sensor [16]. A pneumatic cylinder with a high power-to-weight ratio obviates the need for a reduction gear in order to realize compatibility between adequate torque and high back-drivability, and it also makes the system smaller and lighter. The high back-drivability of the pneumatic actuator allows the detection of external forces from pressure data and compliance control of the system without the use of force sensors.

Earlier prototypes could only present estimated external forces with a sensitivity of around 3 N [16], which is insufficient for the presentation of minute forces generated during surgery to the operator. We have therefore prototyped a new, improved model of surgical manipulators IBIS IV, which has higher performance in the estimation of external forces, and we have conducted experiments to verify its effectiveness.

This paper reports on the developments of and subsequent experiments with the new model surgical manipulators.

Section 2 of this paper describes the mechanism and construction of the new model of pneumatically driven surgical manipulators IBIS IV, which have been newly designed and developed to overcome various issues with conventional models.

Section 3 deals with the configurations of the master-slave system composed of the new model IBIS IV and earlier developed master manipulators. It also deals with its bilateral control.

Section 4 covers the experiments to evaluate the new manipulator model on its performance in estimating external forces. It also covers experimental results of the newly constructed master-slave system.



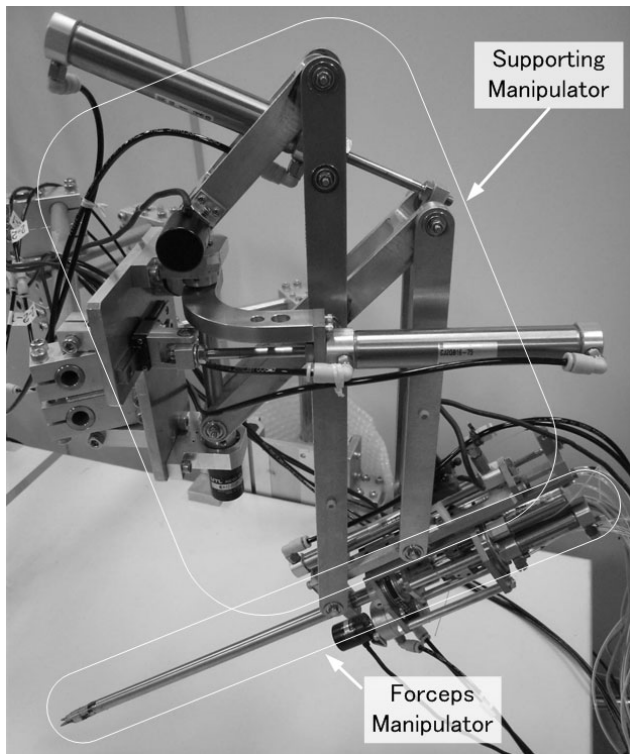


Fig. 1. Newly developed surgical manipulator IBIS IV.

Section 5 provides reflection on the knowledge acquired through this research, and future issues and outlooks.

Section 6 is a summary list of conclusions.

2. Pneumatically Driven Surgical Manipulator IBIS IV

Figure 1 shows the newly designed and developed pneumatic surgical manipulator IBIS IV. The new model IBIS IV, consisting of 2-DOFs forceps manipulators and 4-DOFs supporting manipulators, has 6-DOFs in total. In this system, external forces are estimated from drive forces of the actuator as obtained through back-drivability of the system. Hence, mechanical impedance of the manipulator, including the effects of self-weights, needs to be compensated. Even the accuracy of inverse dynamics model affects to external force estimation, it is almost impossible to create such a perfect model. It becomes critically important, therefore, to minimize mechanical impedance itself by reducing the weight and friction of the manipulator.

With the foregoing taken into consideration, in this prototype, weights of movable parts have been reduced to around one-half of those of the previous prototypes to reduce inertial effects.

Elements of the system are described in detail below.

2.1. Supporting Manipulator

As shown in Fig. 2, the supporting manipulator has 4-DOFs in total, consisting of 3-DOFs in rotation around

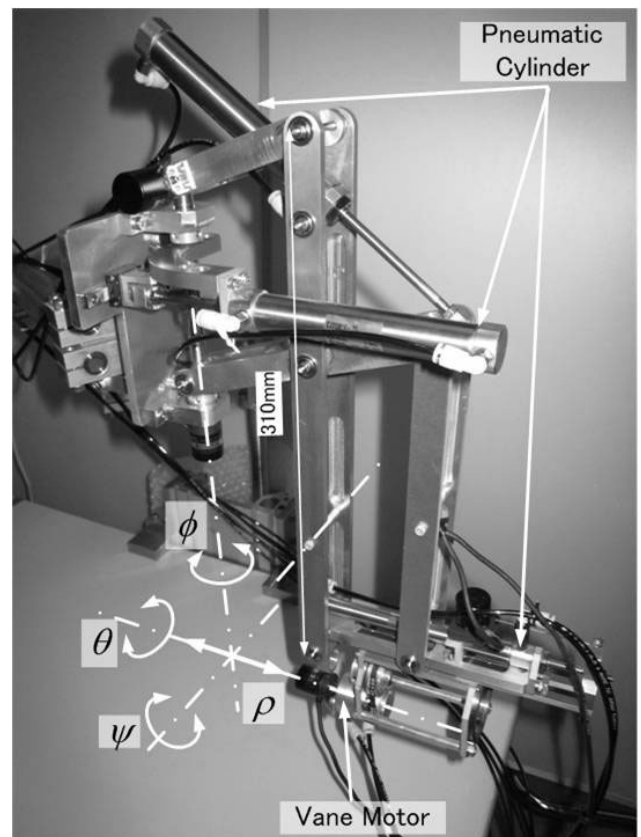


Fig. 2. Supporting manipulator.

the inlet of a trocar cannula and 1-DOF in translation in the direction of forceps insertion. A combination of two sets of parallel link mechanisms and a gimbal mechanism provides a remote center of motion, so that the pivot point at the trocar cannula is mechanically immovable without direct support. Such a mechanism allows actuation of the forceps with minimum loads in-vivo, and it also obviates position-coordinates of the insertion port in the kinematic algorithm.

The ϕ axis is driven by converting linear motions of the cylinder to rotational motions with a slider-rocker mechanism, as shown in Fig. 3. This mechanism, in which the drive cylinder gets inclined together with manipulator as one as ϕ axis rotates, does not protrude outwardly, thus requiring only a minimum of space. The relationship between linear displacement X of the cylinder piston and rotational angle ϕ is expressed as follows:

$$X = d \tan \phi \dots \dots \dots (1)$$

where d denotes distance, as shown in Fig. 3. Joint torques τ_ϕ are obtained from forces F_ϕ of cylinders in accordance with the principle of virtual work as follows:

$$\tau_\phi = \frac{\partial X}{\partial \phi} F_\phi \dots \dots \dots (2)$$

$$= d(1 + \tan^2 \phi) F_\phi \dots \dots \dots (3)$$

On the ψ axis, the slider-crank mechanism has a common axis of rotation with the parallel link mechanism, as shown in Fig. 4, so as to convert linear motions of the

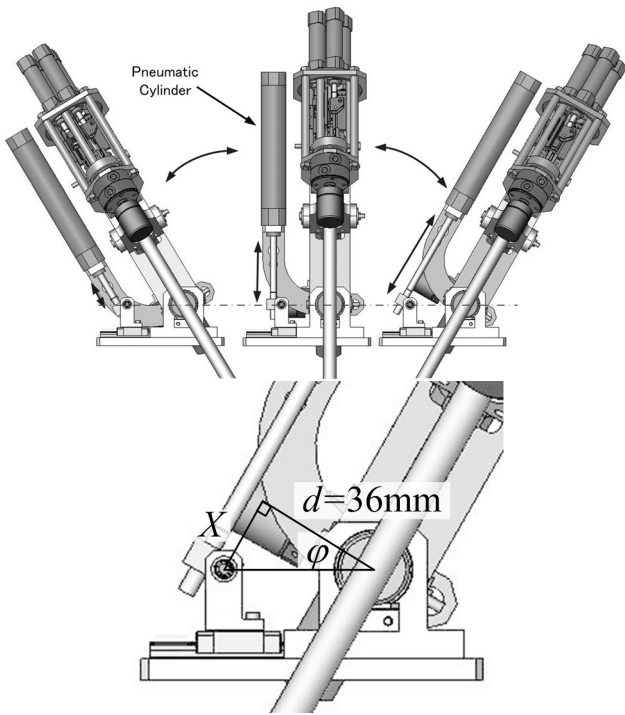


Fig. 3. Design of slider-rocker mechanism for ϕ axis.

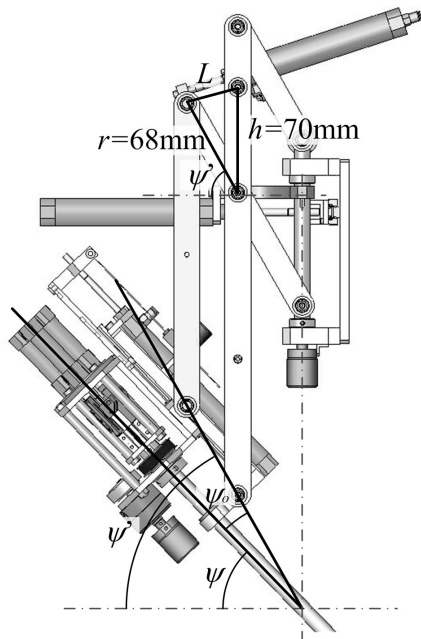


Fig. 4. Design of slider-crank mechanism for ψ axis.

cylinder to rotational motions. Kinematic relations and joint torques are then obtained as follows:

$$L = \sqrt{r^2 + h^2 + 2rh \sin \psi'} \quad \dots \quad (4)$$

$$\tau_\psi = \frac{\partial L}{\partial \psi} F_\psi \quad \dots \quad (5)$$

$$= \frac{rh \cos \psi'}{\sqrt{r^2 + h^2 + 2rh \sin \psi'}} F_\psi \quad \dots \quad (6)$$

$$\psi' = \psi + \psi_0. \quad \dots \quad (7)$$

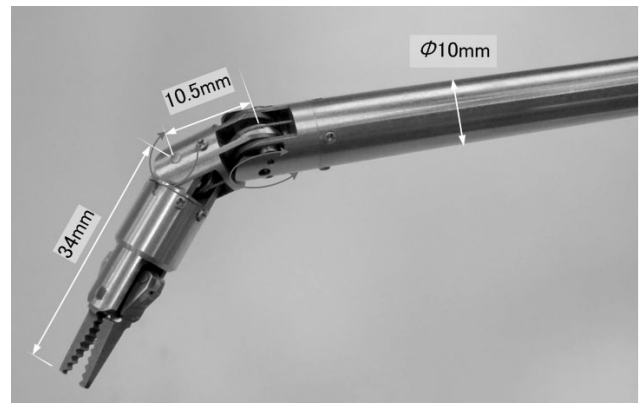


Fig. 5. Tip of forceps manipulator.

where L denotes the distance representing the linear displacement of the cylinder; r and h are constant link parameters. For translation ρ in the direction of the insertion of the forceps, we take linear motions of the pneumatic cylinder.

In this prototype, which has a mechanism similar to that of conventional manipulators, we have set the parameters for the link mechanism as follows with balance between working areas and output torques taken into consideration: $d = 36$ mm, $r = 68$ mm, $h = 70$ mm, tube diameter of pneumatic cylinder on ρ axis = 10 mm, and its stroke = 100 mm.

In addition, we have added a rotating mechanism in the direction of the insertion of the forceps. The mechanism uses a pneumatic rotary actuator to ensure simplified detachment from and attachment to the forceps manipulator. This allows the use of fewer parts in the detachable part, and we have also trimmed excess parts of the links. As a result, the weight of the movable part of the supporting manipulator has been reduced from 2.5 kg to 1.4 kg.

2.2. Forceps Manipulator

The forceps manipulator can make bending of 2-DOFs at the tip, as shown in Fig. 5, and the joints are tendon-driven via stainless wire by the pneumatic cylinder fitted in the rear drive part, as shown in Fig. 6. The wires that drive the second joint are so constrained by guide-rollers 3.4 mm in diameter that they must pass through the rotational center of the first joint. As shown on the schematic drawing of a tendon drive with 1-DOF in Fig. 7, two sets of such tendon-driving systems are installed at right angles to each other about the direction of the forceps insertion.

While the conventional manipulators adopt pneumatic vane motors for driving wires and have rotational freedom about the direction of the insertion of the forceps, this prototype, in which the supporting manipulator has such rotational freedom and pneumatic cylinders drive the tendons, realizes downsizing of the drive part, and this helps reduce the weight of the forceps manipulator from 0.6 kg to 0.2 kg.

Now, we will discuss how to control joint torques τ and mean tensions T_m .

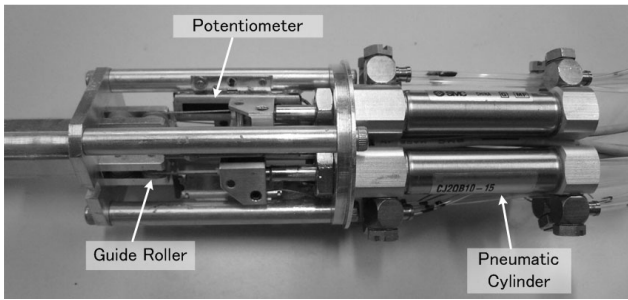


Fig. 6. Drive of forceps manipulator.

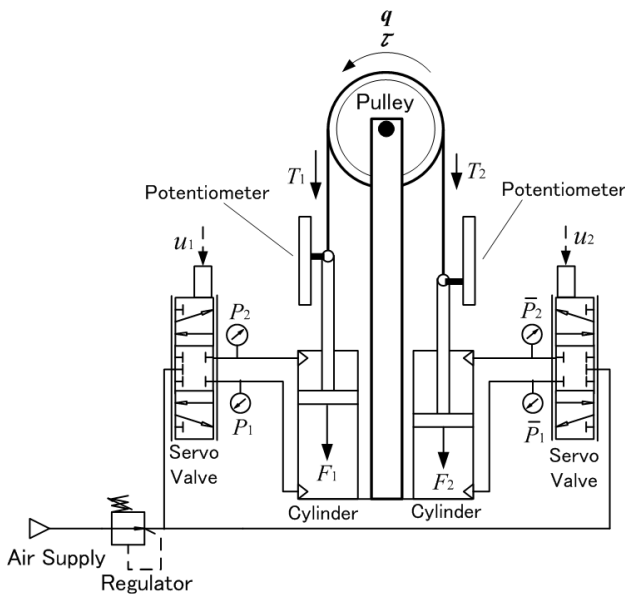


Fig. 7. Schematic view of tendon drive using pneumatic cylinders.

First of all, we can easily obtain static relations geometrically as follows:

$$\tau = r(T_1 - T_2) \dots \dots \dots (8)$$

$$T_m = \frac{T_1 + T_2}{2} \dots \dots \dots (9)$$

where r denotes the radius of the pulley at the forward end, and T_1 and T_2 the tensions of the left and right wires.

T_1 and T_2 are obtained as follows:

$$T_1 = T_m + \frac{\tau}{2r} \dots \dots \dots (10)$$

$$T_2 = T_m - \frac{\tau}{2r} \dots \dots \dots (11)$$

For the tendon drive to be stable will require tension on the wire to be sufficiently strong for it to cause no slack. With minimum tension expressed by T_0 and mean tension by T_m in the following equation:

$$T_m = T_0 + \frac{1}{2}|\tau| \dots \dots \dots (12)$$

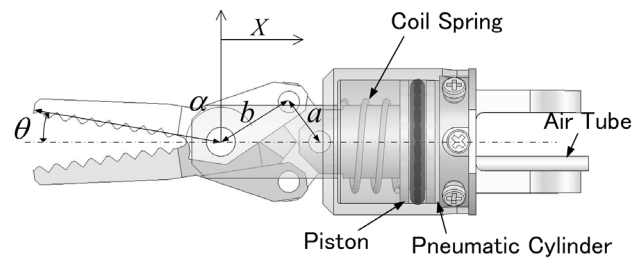


Fig. 8. Schematic drawing of gripper.

then

$$T_1 = T_0 + \frac{|\tau| + \tau}{2r} \geq T_0 \dots \dots \dots (13)$$

$$T_2 = T_0 + \frac{|\tau| - \tau}{2r} \geq T_0 \dots \dots \dots (14)$$

which assures that tensions T_1 and T_2 will be stronger than T_0 . That is to say, if we control wire tension in the way expressed by the Eqs. (13) and (14), we can generate arbitrary drive torques τ while maintaining wire tension at a level of T_0 or above. Assuming that the frictions in pneumatic cylinders are negligible or sufficiently compensated for, T_1 and T_2 will become equivalent to the drive forces of the cylinders. The drive forces of pneumatic actuators are calculated based on measured pressure with pressurized areas of the piston. We have confirmed that a PI control system with a servo valve, feeding back the calculated forces, generated arbitrary drive forces up to about 30 Hz within a supply pressure [17]. The power of the manipulator can be adjusted easily and reliably by reducing the supply pressure.

2.3. Gripping Mechanism

Most conventional multi-DOF-forceps use wire to drive the gripper; wire passed through over plural joints at the risk of interference with other joints. When especially strong gripping forces are to be generated, increased wire tension to drive the gripper will also increase loads on other joints over which the drive wire passes, resulting in changes in the joints' frictional characteristics, etc. In our earlier researches [16] on conventional manipulators using wire to perform open/close actions of the gripper, such interference posed a problem.

We have developed a new gripping mechanism in which a micro pneumatic cylinder and slider-crank mechanism are in combined use to generate strong gripping forces without causing interference to other joints, as shown in Fig. 8. In the newly developed holding mechanism, the pneumatic cylinder is driven by high-pressure air supplied through a polyethylene tube of 1.0 mm in outer diameter and 0.5 mm in inner diameter. It is connected into the hole at the backside of the cylinder; the gripper is closed by the thrust forces of the cylinder and opened by reaction forces of the coil spring.

The relationship between gripper angles θ and linear motional displacements X is expressed by the following

Table 1. Parameters of gripper.

Cylinder diameter	8.5mm
Cylinder stroke	2.3 mm
Spring constant	0.39 N/mm
Link <i>a</i>	3.45 mm
Link <i>b</i>	5.40 mm
α	141°

equation:

$$X = -b \cos(\theta + \alpha) + \alpha \sqrt{1 - \left(\frac{b}{a} \sin(\theta + \alpha)\right)^2} \dots \dots \dots (15)$$

where *a* and *b* denote the lengths of the links, as shown in **Fig. 8**, and α denotes the angles of the links. Torques τ_θ to open and close the gripper are obtained from forces *F* of the cylinder, based on the principle of virtual work, as follows:

$$\tau_\theta = \frac{\partial X}{\partial \theta} F \dots \dots \dots (16)$$

$$= \left(b \sin(\theta + \alpha) - \frac{b \sin(\theta + \alpha) \cos(\theta + \alpha)}{\sqrt{1 - \left(\frac{b}{a} \sin(\theta + \alpha)\right)^2}} \right) F \dots \dots \dots (17)$$

Suture needles are about 0.5–0.7 mm in diameter, and they are held by the gripper at angles of about 12°. If link parameters *a*, *b*, and α are so designed that the denominator of the second member in the parenthesis in Eq. (15) should be asymptotic to zero under the condition, then it become a singular configuration by $\partial X / \partial \theta \rightarrow \infty$ during gripping a needle. Therefore, we will be able to gain a huge τ_θ at small extrusion forces *F* of the cylinders for gripping a needle. This prototype has been designed to the parameters in **Table 1** with gripping forces, working ranges and sizes of the mechanism taken into account. In this case, a singular configuration of $\partial X / \partial \theta = \infty$ is obtained at $\theta = -0.6^\circ$, barely outside the range of movement.

This prototype can generate strong gripping forces of 25 N or more with the gripper in almost closed conditions. Such strong gripping forces are generated without the use of wire for power transmission, hence no loads are generated on other joints.

The part forward of the cylinder can be easily removed to allow repeated cleanings of the inside of the cylinder. The air supply tube can also be removed for replacement. With O-rings made of highly heat-resistant fluoro-rubber materials, the gripper can be sterilized in an autoclave.

3. Master-Slave System

3.1. System Configurations

We have developed a master manipulator capable of displaying sense of force with 6-DOFs [18]. **Fig. 9** shows

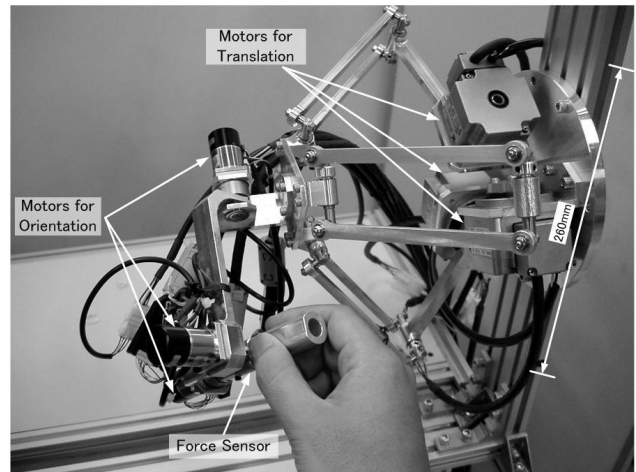


Fig. 9. Developed master manipulator using delta mechanism.

the newly developed master manipulator, in which a delta mechanism for translation and a serial gimbal mechanism for orientation are in combined use to realize a wide working range as well as compactness. As there are no constraints on the fitting sensors in the master manipulator, we have installed a 6-axis, force sensor at the rotational center of the gimbal and have used AC servo motors with built-in Harmonic Drive for the actuator. Thus, we have adopted admittance control for the master manipulator.

The master-slave system consisting of these manipulators is shown in **Fig. 10**. Communications between master and slave are based on UDP/IP, which we have confirmed may cause a delay of 1 ms or less on local networks.

3.2. Bilateral Control by Impedance Control

One of the objectives in the control of the master-slave system is to realize high degrees of transparency by making identical positions and forces for master and slave manipulators on the task coordinate system, irrespective of environments [19, 20]. Such an ideal system could provide a feel to the operator as if the task were hands-on. Then, the accuracy and safety of the task would completely depend on the operator’s skills. This would mean that any unexpected generation of excessive velocities or forces, or any trembling of the hands, would be reproduced in the slave manipulator owing to the high transparency of the system.

In our master-slave system, we have applied compliance control to the slave manipulator to take advantage of flexibility and back-drivability of the pneumatic drive. This will help prevent excessive loads from generating in-vivo, but may cause positional deviations between the master and slave manipulators. Generally, however, operators do not look at one’s hands or the master manipulator during the task, but they get visual feedback on positions of the slave manipulator on the monitor, without any particular odd feelings. On the other hand, the master manipulator is provided with appropriate viscosity effects to constrain any trembling of the hands or the generation of excessive velocities.

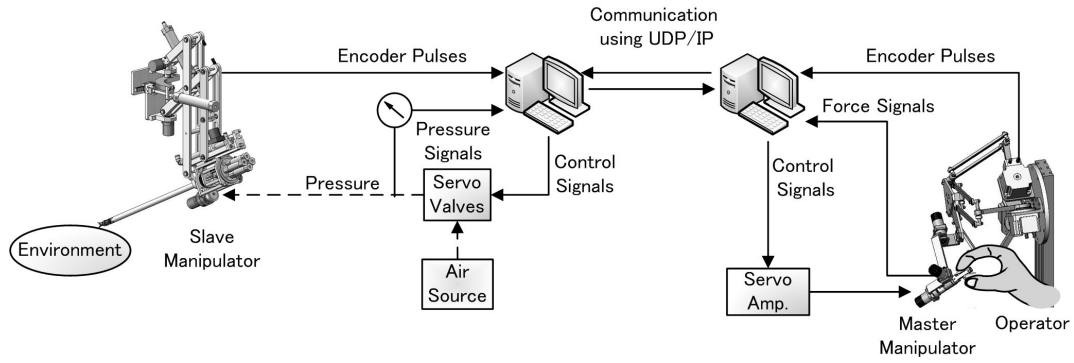


Fig. 10. Developed master-slave system.

Based on the above-mentioned consideration, master and slave manipulators are so controlled as to be provided with the following impedance characteristics.

$$\text{slave : } -f_s = M_s \ddot{r}_s + B_s (\dot{r}_s - \dot{r}_m) + K_s (r_s - r_m) \dots \dots \dots (18)$$

$$\text{master : } f_m - f_s = M_m \ddot{r}_m + B_m \dot{r}_m \dots \dots \dots (19)$$

where,

- $r_s \in \mathbf{R}^{6 \times 1}$: Positional vector of the forward tip of the slave
- $r_m \in \mathbf{R}^{6 \times 1}$: Positional vector of the forward tip of the master
- $f_s \in \mathbf{R}^{6 \times 1}$: Forces applied to environments by the forward tip of the slave
- $f_m \in \mathbf{R}^{6 \times 1}$: Forces applied to the master by operators
- $M_s \in \mathbf{R}^{6 \times 6}$: Set inertia for the slave
- $M_m \in \mathbf{R}^{6 \times 6}$: Set inertia for the master
- $B_s \in \mathbf{R}^{6 \times 6}$: Set viscosity for the slave
- $B_m \in \mathbf{R}^{6 \times 6}$: Set viscosity for the master
- $K_s \in \mathbf{R}^{6 \times 6}$: Set rigidity for the slave

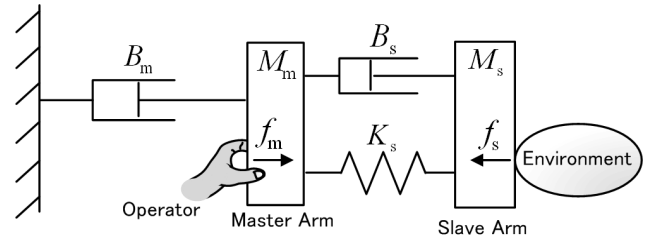


Fig. 11. Conceptual model of impedance-controlled master-slave system.

Figure 11 shows a 1-axial conceptual model of an impedance-controlled master-slave system. As shown in Fig. 12, the slave manipulator is controlled by impedance control with internal force-control loops, and the master manipulator, by admittance control. “Pneumatic Force Controller” and “Motor Driver” in Fig. 12 respectively refer to the PI controller for the drive force of the pneumatic actuator and to the PID controller for angular velocities by the motor driver. Function Z represents an inverse dynamics model of the slave manipulator, where reference drive forces f_{ref} on the slave side are dealt with as estimated external forces to be transmitted to the master side.

4. Experimental Results

4.1. Experiments to Estimate External Forces

We have conducted experiments with the IBIS IV to evaluate its performance in estimating external forces.

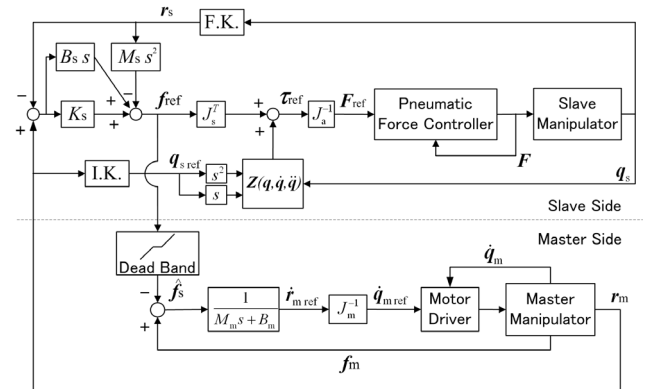


Fig. 12. Block diagram of bilateral control.

The experiments have been conducted with the system in which the control systems in Fig. 12 are implemented and with drive forces f_{ref} taken for external forces f_{ext} . In the experiments, we have established the following settings: $M_s = 0.1$ kg, $B_s = 0.02$ Ns/mm, and $K_s = 0.4$ N/mm.

In the first experiment, we let the forceps move freely to the reference positions of a sinusoidal wave without contact with external environments. Estimated external forces as obtained through the experiment are shown in Fig. 13. Ideally, estimated external forces during free motions should be 0 N, but in practice there are some errors of around ± 1.0 N at the maximum. In transmitting force-data to the master, therefore, the force-data need to be passed through a threshold filter, which cuts off signals with an absolute value less than 1.0 N, so that such

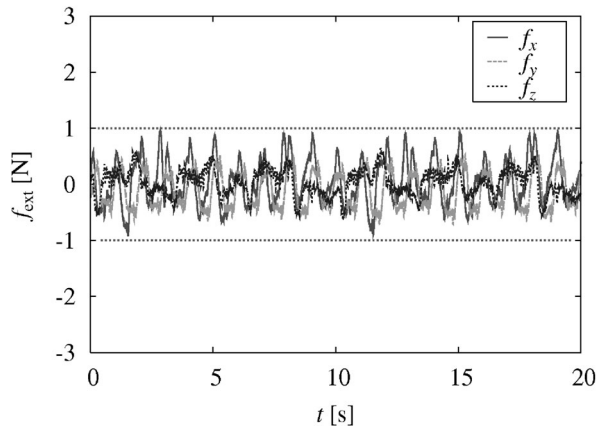


Fig. 13. Estimated external force during free motion.

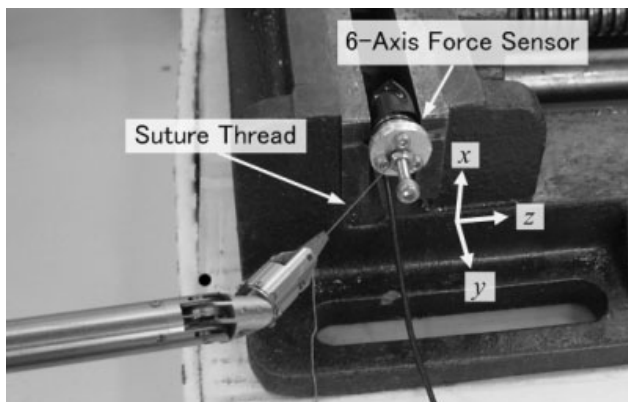


Fig. 14. Experimental setup.

errors in estimation could be filtered and not transmitted to the master. Consequently, the system's sensitivity to forces is 1.0 N. Such errors in estimation, which probably represent errors of the inverse dynamics model of the manipulator, are fewer than conventional prototypes by 50% or more, thus proving improvements in performance. Further improvement in sensitivity to detect much more minute forces will require further lightening of the system and further improvement of the dynamics model.

In the second experiment, we have compared, against estimated forces, output of the force sensor when suture thread in the fixed force sensor is held and pulled by the forceps manipulator, as shown in Fig. 14. In the experimental results, shown in Fig. 15, errors are within around 0.5 N, indicating that output of the force sensor corresponds considerably well to the values estimated by the IBIS IV. These errors are considered mainly due to frictional forces of the mechanism. In the future, therefore, we need to reduce friction further.

4.2. Experiments on Bilateral Control by Impedance Control

With the above-mentioned system in which impedance parameters are set as per Table 2, we have carried out a suturing task on a dummy organ, as shown in Fig. 16. Fig. 17 shows a part of the experimental results with re-

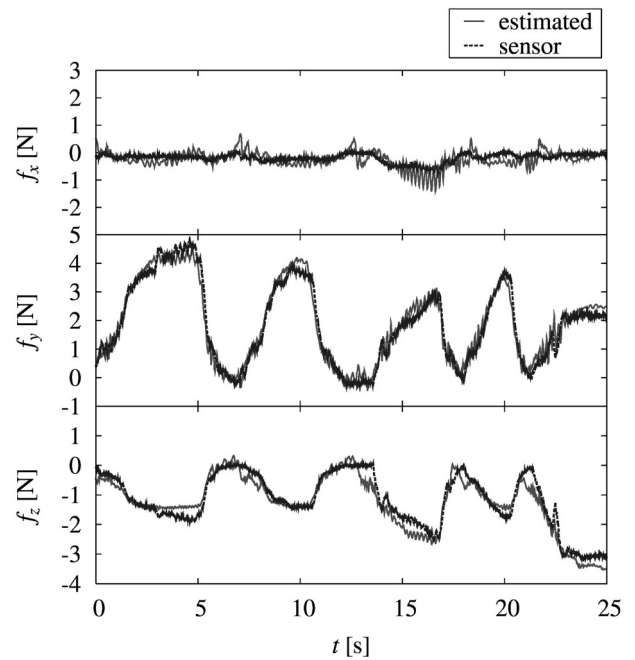


Fig. 15. Comparison between estimated force and sensor output.

Table 2. Impedance parameters.

M_s	0.02	kg
M_m	1.0	kg
B_s	0.02	Ns/mm
B_m	0.009	Ns/mm
K_s	0.6	N/mm

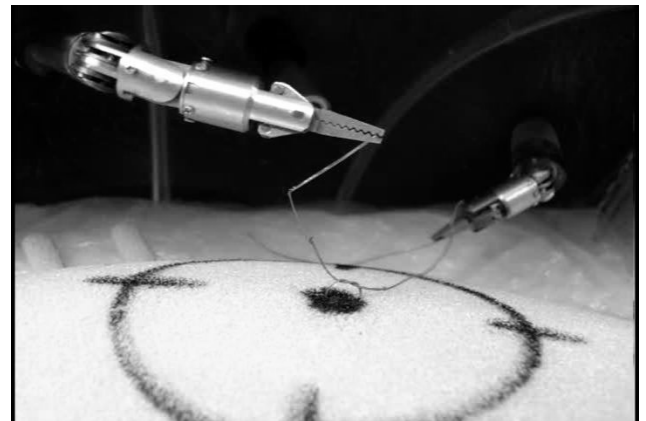


Fig. 16. Suturing experiment.

spect to y-axial responses of positions and forces for the master and slave manipulators; the operator is handling the thread to form a knot until approximately 60 s. During this time, there are almost no forces generated and the slave manipulator follows up the master manipulator very closely in positions. In the lapse of about 60 s, the operator has started pulling the thread and tightening knots, at which time there are forces of as much as 2 N generated. Positional deviations of the master and slave manipulators are proportional to external forces as per the set values of stiffness K_s , and the master and slave manipulators

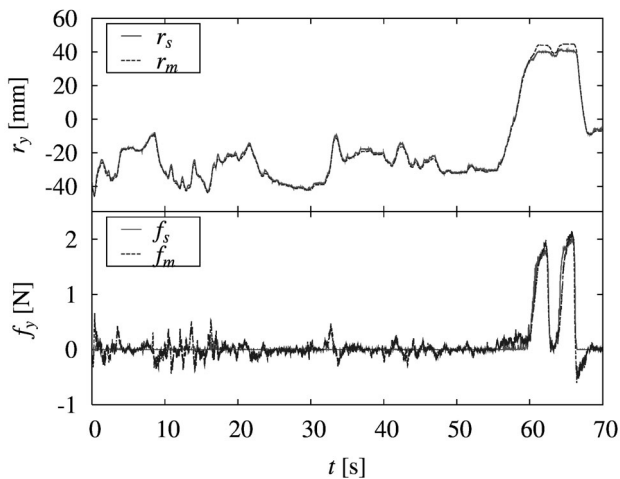


Fig. 17. Experimental results of bilateral control.

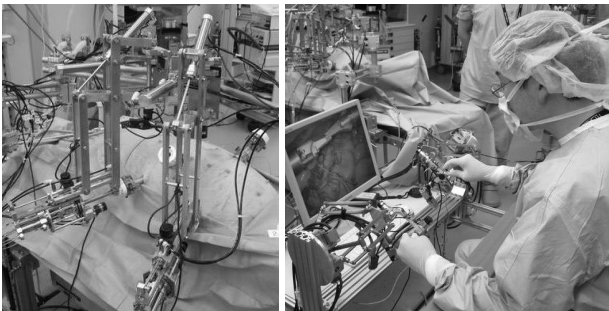


Fig. 18. In-vivo experiment.

present practically identical forces, suggesting that thread tensions are adequately fed back to the operator.

4.3. In-Vivo Experiments

We have conducted, using the developed master-slave system, in-vivo experiments on a pig, as shown in Fig. 18. The experiments had the following objectives:

- to confirm the motions of the manipulators in intra-abdominal environments,
- to confirm setting up procedures in surgical sites, and
- to obtain data on forces in in-vivo environments.

We have carried out the task of pushing a needle into the liver and intestines and then suturing them under pneumoperitoneum.

We have found from the experiments that the forward tip of the manipulator, in particular the gripping mechanism, works very well in handling the curved needle at strong gripping forces without any adverse effects from body fluids. The suturing task in the abdomen was smoothly accomplished by the operator. Against concerns about possible deviations in positions between the remote center of motion of the manipulator and the actual insertion point due to respiration or changes in abdominal air pressure, in practice, no deviations in position have been observed when the forceps manipulator is inserted.

While there is no abdominal gas leakage observed through the forceps manipulator, some body fluids are pushed out from the abdomen by capillarity or abdominal air pressure, and they have run along the wire path into the potentiometer that measures angles of the forward end joint. This has caused too much noise in displacement measurements to obtain favorable results in estimations of external forces.

5. Discussion

5.1. Force Sensitivity

The proposed surgical manipulator, in which external forces can be estimated through the use of the back-drivability of the pneumatic actuator, is susceptible to effects of the dynamics of the manipulator itself, such as friction and inertia. How to mitigate such effects, therefore, is an essential issue. In this research, we have reduced the weight of the movable part of the manipulator to mitigate effects of inertia and friction, and thereby to reduce absolute errors of the dynamics model. As a result, about a 50% reduction in the weight of the movable part has improved sensitivity to external forces to about 1.0 N, an increase of at least 50%.

A sensitivity of 1.0 N is considered sufficient to sense the tensions in tightening suturing thread, according to reference [11] and in-vitro experimental results. This degree of sensitivity, however, is not enough to get a feel when soft organs are lightly pushed down. We therefore need to further improve force sensitivity of the manipulator in the future. Further miniaturization and lightening of the manipulator will enable it to estimate external forces to a much higher degree of sensitivity. At the same time, we may have to quantitatively evaluate and clarify the actual relations between force sensitivity and the efficiency/safety of the task in the future.

5.2. Behaviors in In-Vivo Environments

In the in-vivo experiments, we confirmed that the machine can successfully perform suturing tasks in the abdomen of the subject. However, we also experienced a new problem – that of significant noise in the measurements of displacements due to body fluids running out of the abdomen, along the forceps, and into the potentiometer. The problem may be resolved by devising wire paths so that water does not reach the potentiometer or by changing the construction so that the water is let out in other ways.

Respiration might cause slight changes in loads applied to the manipulator at the insertion point, although no deviations are observed in positions between the remote center of motion of the manipulator and the actual insertion point. At this moment, such effects of respiration may be negligibly small as compared to errors of the dynamics model, but in the future when the manipulator is further improved to make it much more sensitive to inner force, such small effects may have to be addressed as well.

As for sterilizing and cleaning the manipulator, the part of the prototype forceps manipulator that contains the pneumatic cylinders and potentiometers is detachable, as shown in Fig. 6, to allow it to be cleaned and sterilized in an autoclave. The supporting manipulator and the drive part of the forceps manipulator that contains the actuators and potentiometers are so heat resistant that they can be sterilized by ethylene oxide gas. However, cleaning treatments may affect the potentiometers and encoders. Therefore, at present, they need to be covered with a drape during operation.

5.3. Safety and Risks Involved in Operation

The ingress of water into the potentiometer as described above may not only cause deterioration of control performance but also risks of fault current. To avoid such inconveniences, energized parts need to be properly isolated, and drive parts need to be made of non-conductive materials such as engineering plastics. This will also make the drive parts lighter.

The forceps manipulator we have developed uses wire to drive the bending joints. The wire, though sufficiently strong against forces generated by the pneumatic cylinders, is at risk of breaking at the bend due to flexure fatigue. In the tendon-driving system of the forceps manipulator developed, displacements are redundantly measured by the potentiometers fitted to the wires on both sides. Consequently, any broken wire may be detected by checking the alignments in the readings of both potentiometers. Still, if huge tensions are applied to the unbroken wire in a pair, the bending joints will momentarily rotate at high speed, involving a risk of delayed detection of broken wires. We need to take countermeasures against such problems.

On the other hand, pneumatic servo systems can not only limit, by regulating supply pressure, the maximum force generated by the manipulators in an easy and sure way; they can also make the manipulators come to an emergency stop by arranging an electromagnetic valve between the pneumatic actuator and servo valve in such a way that it operates in the event of power failure or other anomalous occurrence. In these systems, we can choose whether forces are let off or retained in each joint by exhausting or shut off compressed air in the actuator.

We need to study such emergency operations further in the future.

6. Conclusions

This paper presents a new, enhanced model IBIS IV, a pneumatically driven surgical manipulator we have developed as a prototype. Through the experiments to evaluate its performance in estimating external forces, we have confirmed that the newly developed model can estimate external forces with a sensitivity of around 1.0 N without the use of force sensors. We have also confirmed that the newly constructed master-slave system can convey the

tension on suturing thread to the operator in an appropriate way. We have confirmed through in-vivo experiments that suturing tasks can properly be performed on the abdomen. Notwithstanding these achievements of the newly developed model, we still have the following issues to be addressed in the future: improvement in the basic performance of the pneumatically driven forceps manipulators, as well as the solution of various problems involved and evaluations of their operability and safety, depending on the availability of force-feedbacks and changes in the scaling of set impedances, positions, and forces.

Acknowledgements

This research has been conducted through financial support from official scientific research funds 21760190 and 21360114.

References:

- [1] R. H. Taylor and D. Stioianovici, "Medical Robotics in Computer-Integrated Surgery," *IEEE Trans. on Robotics and Automation*, Vol.19, No.5, pp. 765-780, 2003.
- [2] H. Yamashita, D. Kim, N. Hata, and T. Dohi, "Multi-Slider Linkage Mechanism for Endoscopic Forceps Manipulator," In Proc. of the 2003 IEEE/RSJ, Int. Conf. on Intelligent Robots and Systems, Vol.3, pp. 2577-2582, 2003.
- [3] N. Matsuhira et al., "Development of a Functional Model for a Master-Slave Combined Manipulator for Laparoscopic Surgery," *Advanced Robotics*, Vol.17, No.6, 2003, pp. 523-539.
- [4] M. Hashizume et al., "Early Experience of Endoscopic Procedures in General Surgery Assisted by a Computer-Enhanced Surgical System," *Surgical Endoscopy*, Vol.16, 2002, pp. 1187-1191.
- [5] M. C. Cavusoglu, W. Williams, F. Tendick, and S. S. Sastry, "Robotics for Telesurgery: Second Generation Berkeley/Ucsf Laparoscopic Telesurgical Workstation and Looking Towards the Future Applications," In Proc. of the 39th Allerton Conf. on Communication, Control and Computing, Oct. 2001.
- [6] F. Tajima, K. Kishi, K. Nishizawa, K. Kan, H. Ishii, M. G. Fujie, T. Dohi, K. Sudo, and S. Takamoto, "A Prototype Master-Slave System Consisting of Two MR-Compatible Manipulators with Interchangeable Surgical Tools," In Proc. of Int. Conf. on Robotics and Automation, 2004.
- [7] J. Arata, M. Mitsuishi, S. Warisawa, K. Tanaka, T. Yoshizawa, and M. Hashizume, "Development of a Dexterous Minimally-Invasive Surgical System with Augmented Force Feedback Capability," In Proc. of Int. Conf. on Intelligent Robots and Systems, pp. 3738-3743, Aug. 2005.
- [8] M. J. H. Lum, D. Trimble, J. Rosen, K. Fodero II, H. H. King, G. Sankaranarayanan, J. Doshier, R. Leuschke, B. M. Anderson, M. N. Sinanan, and B. Hannaford, "Multidisciplinary Approach for Developing a New Minimally Invasive Surgical Robotic System," In Proc. of the 2006 BioRob Conf., 2006.
- [9] O. Gerovichev, P. Marayong, and A. M. Okamura, "The Effect of Visual and Haptic Feedback on Computer-Assisted Needle Insertion," *Computer-Aided Surgery*, Vol.9, No.6, 2004, pp. 243-249.
- [10] J. T. Dennerlein, D. B. Martin, and H. Zak, "Haptic Force-Feedback Devices for the Office Computer: Performance and Musculoskeletal Loading Issues," *Human Factors*, Vol.43, No.2, 1996, pp. 278-286.
- [11] A. M. Okamura, L. N. Verner, C. E. Reiley, and M. Mahvash, "Haptics for Robot-Assisted Minimally Invasive Surgery," In Proc. of the Int. Symposium Robotics Research, Hiroshima, Japan, November 26-29, 2007.
- [12] G. Tholey, J. P. Desai, and A. E. Castellanos, "Force Feedback Plays a Significant Role in Minimally Invasive Surgery," *Annals of Surgery*, Vol.241, No.1, 2005, pp. 102-109.
- [13] M. Kitagawa, D. Dokko, A. M. Okamura, and D. D. Yuh, "Effect of Sensory Substitution on Suturemanipulation Forces for Robotic Surgical Systems," *The J. of Thoracic and Cardiovascular Surgery*, Vol.129, No.1, 2005, pp. 151-158.
- [14] S. Tachi, T. Sakaki, H. Arai, S. Nishizawa, and J. F. Pelaez-Polo, "Impedance Control of a Direct-drive Manipulator without Using Force Sensors," *Advanced Robotics*, Vol.5, No.2, 1991, pp. 183-205.
- [15] A. J. Madhani, G. Niemeyer, and J. K. Salisbury Jr., "The Black Falcon: A Teleoperated Surgical Instrument for Minimally-Invasive Surgery," *Proc. of IEEE/RSJ Int. Conf. on Intelligent Robotic Systems*, Vol.2, pp. 936-994, 1998.

- [16] K. Tadano, K. Kawashima, and T. Kagawa, "Evaluation of a Master Slave System with Force Sensing," Proc. of SICE Annual Conf., pp. 2871-2874, 2007.
- [17] K. Tadano, K. Kawashima, and T. Kagawa, "Development of Robot Manipulator for Laparoscopic Surgery with Force Display Using Pneumatic Servo System," Proc. of 7th JFPS Int. symposium on Fluid Power, pp. 821-824, 2008.
- [18] K. Tadano and k. Kawashima, "Development of 4-DOFs Forceps with Force Sensing Using Pneumatic Servo System," Proc. of IEEE/ICRA, 2006, pp. 2250-2256.
- [19] Y. Yokokohji and Y. Yoshikawa, "Bilateral Control of Master-Slave Manipulators for Ideal Kinesthetic Coupling," IEEE Trans. on Robotics and Automation, Vol.10, No.5, 1994, pp. 605-620.
- [20] B. Hannaford, "Design Framework for Teleoperations with Kinematic Feedback," IEEE Tanas. on Robotics and Automation, Vol.5, pp. 426-434, 1998.



Name:
Kotaro Tadano

Affiliation:
Assistant Professor, Precision and Intelligence Laboratory, Tokyo Institute of Technology

Address:
4259 Nagatsuta, Midori-ku, Yokohama-shi 226-8503, Japan

Brief Biographical History:
2007 Completed Doctoral Course in mechanical engineering at Tokyo Institute of Technology
2007- Special Researcher, Tokyo Institute of Technology
2008- Assistant Professor, Tokyo Institute of Technology

Main Works:
• "Development of a Master Slave Manipulator with Force Display using Pneumatic Servo System for Laparoscopic Surgery," Int. J. of Assistive Robotics and Mechatronics, Vol.8, No.4, pp. 6-13, 2007.

Membership in Academic Societies:
• The IEEE Robotics and Automation Society (IEEE-RAS)
• The Japan Society of Mechanical Engineers (JSME)
• The Robotics Society of Japan (RSJ)



Name:
Kenji Kawashima

Affiliation:
Associate Professor, Precision and Intelligence Laboratory, Tokyo Institute of Technology

Address:
4259 Nagatsuta, Midori-ku, Yokohama-shi 226-8503, Japan

Brief Biographical History:
1997-2000 Research Assistant, Department of Mechanical Engineering, Tokyo Metropolitan College of Technology
2000- Associate Professor, Precision and Intelligence Laboratory, Tokyo Institute of Technology

Main Works:
• "Application of Robots Using Pneumatic Artificial Rubber Muscles for Operating Construction Machines," IEEE/IROS, Vol.4, pp. 3384-3389, 2003.

Membership in Academic Societies:
• The Japan Society of Mechanical Engineers (JSME)
• The Robotics Society of Japan (RSJ)
• The Japanese Society of Instrumentation and Control Engineers (SICE)



Name:
Kazuyuki Kojima

Affiliation:
Assistant Professor, M.D., Ph.D., Surgical Oncology, Graduate School of Medicine, Tokyo Medical and Dental University

Address:
1-5-45 Yushima, Bunkyo-ku, Tokyo 113-8519, Japan

Brief Biographical History:
1999- Staff, Second Surgery, Tokyo Medical and Dental University
2003- Assistant Professor, Second Surgery, Tokyo Medical and Dental University
2005- Assistant Professor, Surgical Oncology, Tokyo Medical and Dental University

Main Works:
• "A Comparison of Roux-en-Y and Billroth-I Reconstruction After Laparoscopy-assisted Distal Gastrectomy," Annals of Surgery, Vol.247, pp. 962-967, 2008.

Membership in Academic Societies:
• Japan Surgical Society (JSS)
• Japan Society For Endoscopic Surgery (JSES)
• Japan Gastric Cancer Association (JGCA)



Name:
Naofumi Tanaka

Affiliation:
Director, Operation Center, University Hospital Faculty of Medicine, Tokyo Medical and Dental University

Address:
1-5-45 Yushima, Bunkyo-ku, Tokyo 113-8519, Japan

Brief Biographical History:
1990 Graduated from School of Medicine, Shinshu University
1990- Joined Department of Anesthesiology of TMDU
1995- Belonged to Operation Center
2005- Director of Operation Center

Main Works:
• "Wavelet-Based Compression and Segmentation of Hyperspectral Images in Surgery," Springer Lecture Notes in Computer Science (LNCS) Vol.5125, pp. 142-149, 2008.

Membership in Academic Societies:
• Japanese Association for Operative Medicine (JAOM)
• Japanese Society of Anesthesiologist (JSA)
• Japanese Society of Mechanical Engineering (JSME)